

ESTA/CoRoT Task 1 - Models Comparison

Preliminary results

Monteiro M.J.P.F.G. (Porto)
 Castro M. (Toulouse)
 Christensen-Dalsgaard J. (Aarhus)
 Del'Innocenti S. (Pisa)
 Lebreton Y. (Paris)
 Marconi M. (Napoli)
 Montalbán J. & BAG (Liège)
 Morel P. (Nice)
 Prada Moroni P.G. (Pisa)
 Teixeira T.C. (Porto & London)

Abstract

In this poster we present the first results on Task 1 for the Evolution and Seismic Tools Activity (ESTA) within the CoRoT mission. Several target stars have been identified and models produced with different codes have been calculated to represent the target stars.

A description of the Codes being used to calculate the models as well as their results for the targets proposed are presented. Global parameters as well as the internal structure are compared in order to identify the major differences between the codes being used.

A discussion on the possible origin of the differences is provided. A brief discussion on the *work-to-be-done* is also included.

1 Evolution Codes

Here a brief description of the Evolution codes being used is included and/or the references where those descriptions can be found are provided. The codes whose results will be presented in the next sections are: ASTEC, CESAM, CLES, FRANEC and TGECC.

1.1 ASTEC - Aarhus Stellar Evolution Code [*Christensen-Dalsgaard*]

There has unfortunately not been time to implement with care all the proposals of Mario for the comparison models. Even so I hope that the comparison will provide some indications of where improvements in the ASTEC code are required. Some progress on bringing the modelling into accordance with the specifications will certainly be made before the next CoRoT week. I also expect that the discussions in Toulouse will lead to refinement of the specifications.

The only general description of the code available in print is unfortunately still Christensen-Dalsgaard (1982, CD82 in the following). (Further details are available, but hardly accessible, in Christensen-Dalsgaard 1978). Needless to say, the code has been substantially developed since, particularly (with regards to the present comparison) in including other treatments of opacity, equation of state and nuclear reactions, and inclusion of treatment of the convective core. (A further addition, undoubtedly to be tested later, is the inclusion of diffusion and settling.) However, the basic numerical scheme is at least as set out by CD82.

Numerics:

The models start from the ZAMS (PMS evolution has been used in the code, but not tested with care).

As presented by CD82, the chemical evolution is integrated with the general solution of the structure and evolution equations. However, a separate treatment is used for the chemical evolution of the convective core, using the averaged reaction rates. This is carried out in parallel with the Henyey iteration, although occasionally with fixes to ensure convergence (freezing the properties of the core).

The scheme for defining the mesh is broadly as described by CD82; however, a very dense mesh is used near the boundary of a possible convective core. The present calculations used 601 points (between centre and photosphere).

The timestep is set based on relative (or \log_{10}) changes in several quantities being limited to be below a specified limit (in the present calculations 0.1). Changes in the hydrogen abundance in a convective core are scaled by a factor 5, to compensate for the rather crude numerical treatment of the core composition. As a result, more timesteps are used in models with a convective core. In the present case, typically 200 steps are required to reach exhaustion of hydrogen at the centre, in models with a convective core, and 30 - 40 steps in a model without (this small number is also a consequence of the crude treatment of the nuclear network; see below).

Equation of state:

OPAL 2001 tables, for the appropriate value of Z ($=0.02$ or 0.01). Using the OPAL interpolation scheme.

Opacity:

OPAL 1996 tables, with Alexander low-temperature values. Houdek interpolation scheme. The heavy-element abundance is taken to be the initial value, regardless of the changes due to nuclear reactions. (In models with diffusion and settling, these effects on heavy elements are decoupled from

the nuclear changes in composition, for now. The modified heavy-element abundance is used for the opacity but not, usually, for interpolated equations of state.)

Energy generation:

Nuclear reaction parameters generally from Bahcall & Pinsonneault (1995). (Needs changing for consistency with specifications.) Salpeter weak screening.

³He is assumed to be in nuclear equilibrium at all times.

The CN part of the CNO cycle is assumed to be in nuclear equilibrium at all times, with an initial ¹⁴N abundance taken to include also the original ¹²C abundance. The conversion of ¹⁶O into ¹⁴N is taken into account. The initial abundance of ¹⁴N and ¹⁶O, relative to the heavy-element abundance, are 0.2337 and 0.5154. (May well need to be changed, to meet specifications.)

Convection treatment:

Böhm-Vitense (1958) mixing-length treatment, probably with Henyey et al. (1965) detailed parameters. (The specification of these parameters seems a little uncertain.) Turbulent pressure is not included.

Atmosphere:

Integration of hydrostatic equation assuming the grey Eddington $T(\tau)$ relation:

$$T = T_{\text{eff}} \left[\frac{3}{4} \left(\tau + \frac{2}{3} \right) \right]^{0.25},$$

starting at $\tau=0.01$ and matching where $T=T_{\text{eff}}(\tau=2/3)$. (Note that there are potential problems with the treatment of radiation pressure in the atmosphere, certainly for relatively massive (and hot) stars.)

1.2 CESAM - Code d'Évolution Stellaire Adaptatif et Modulaire [Lebreton & Morel]

The only one published general description in English of the code available in print is Morel (1997). A detailed description (in French) of the previous F77 version is available under request at the WEB sites:

<http://www.obs-nice.fr/morel/CESAM>
<http://www.obs-nice.fr/cesam/>

An abridged “mode d’emploi” (Instructions for use) and the source of the evaluation version of the F95 CESAM2k code used for the present CoRoT Task 1 Models comparison Project, are available on anonymous FTP:

<ftp://ftp.obs-nice.fr/pub/morel/depot/CESAM>

For the present project neither the diffusion of chemical species and/or of the angular momentum are used.

There are two versions of CESAM2k. The first one, the “official” CESAM2k_V0 (in the following, CESAM₀) is no more than an improved version of the former – CESAM2 to CESAM5. It uses the programming facilities offered by F95. About the physics there is no fundamental change.

The main difference with second version (in the following, CESAM₁), used also here for the comparisons, is the introduction of the diffusion of angular momentum. In doing that, some numerical changes and/or improvements have also been done on necessity. With solid rotation, as for the

CoRoT Task 1 comparisons, the two codes are equivalent. (The improved version, actually named CESAM2k_V1.4, though in evaluation, is available on simple request to Pierre.Morel@obs-nice.fr.)

Numerics:

The so called semi-spectral method is used for solving the two points boundary initial value differential problem of stellar evolution. The unknowns are represented by piecewise polynomials. The order of the polynomials and the degree of the oscularity at the connections are fixed accordingly to the required accuracy. The lowest one is equivalent to the centred finite differences scheme. The piecewise polynomials are projected on a basis of normalised B-splines. The implicit non-linear differential problems are iteratively solved for the coefficients of B-splines with the basic Newton-Raphson algorithm (Henyey method). Iteratively until convergence, the chemical composition is updated then, the internal structure and atmosphere equations are solved with the new estimated chemical composition (so-called method of lines). The internal structure and atmosphere equations are solved by collocation. Without diffusion the chemical composition is obtained using an implicit Runge-Kutta scheme specially designed for stiff differential problems. (The implicit parabolic differential problems of the diffusion of chemical species and of the angular momentum are solved with finite element method.)

The models are initialised either from the ZAMS “zero age homogeneous main sequence” or from a homogeneous PMS model in quasi-static equilibrium with a central temperature close to 6×10^5 K.

The mixing of convective zones is made simultaneously with the temporal integration of chemical species. Any limit between a convective and a radiative zone is automatically pushed towards the closest grid point, there discontinuities of the chemical species are set (with diffusion the discontinuities only affect the first derivatives).

The zoning is made by an automatic grid generation, the number of shells varies accordingly to the kind of accuracy required and, along the evolution, in order to limit the change of variables between any grid point to the next. The present calculations use the “corot” accuracy. There between the centre and the upper limit of the envelope from 1030 points (Case 1.1) to 1300 points (Case 1.5). The atmosphere is restored on a grid of 100 points.

The time step is set based on the relative changes of hydrogen. No convergence of any iterative algorithm halved the time step.

Equation of state:

OPAL 2001 EoS tables are used with the OPAL interpolation scheme for tables with $Z=0.01$ or $Z=0.02$, accordingly to the initial value of Z .

Opacity:

OPAL 1996 opacity tables are used, with Kurucz low-temperature values. The heavy-element abundances are taken to be the initial values, regardless of the changes due to nuclear reactions.

Energy generation:

Basic PP + CNO nuclear reactions network is used with ⁷Li, ⁷Be, ²H at equilibrium, even for Case 1.4 initialised at PMS. The nuclear reaction rates are computed using the formula of the NACRE compilation (other compilations and networks are available). The initial abundance of each chemical species is split between its isotopes according to the isotopic ratios of nuclides. Initial ²H is already

assumed to be converted into ${}^3\text{He}$.

Salpeter weak screening is used.

Convection treatment:

The classical Böhm-Vitense mixing-length treatment Böhm-Vitense (1958) taking into account the optical thickness of the convective bubble is used with standard parameters.

Atmosphere:

Integration of hydrostatic equation assuming a $T(\tau)$ relation based on the grey Hopf atmospheric law, starting at $\tau=1\times 10^{-4}$. For the CoRoT Task 1 models, the connection with the envelope is made at $\tau=10$ there, the continuity of the variables and of their first derivative with respect to the space is insured. The radius of the star is assumed to be the bolometric one, i.e. the radius at the level where the local temperature is equal to the effective temperature (close to $\tau=0.65$ with the Hopf's law).

1.3 CLES - Code Liègeois d'Evolution Stellaire [*Scuflaire & BAG*]

CLES is still in an active phase of development at the Institute of Astrophysics of Liège. Some choices that have been made are still subject to changes.

Numerics:

Clés is a lagrangian code. Finite difference equations of order two are used for the discretization of the spatial equations. The mesh size is automatically adapted so as to limit the variations of physical variables from one mesh to the next one. The finite difference scheme written to follow the time evolution is of order one in the abundances in order to avoid numerical instabilities. The timestep is chosen to limit the variations of the physical variables from one model to the next. It is also reduced when the convergence of the resolution or the spatial equations becomes too slow.

The evolution sequences are normally started on the Hayashi sequence.

Equation of state:

Two equations of state are implemented, CEFF (Christensen-Dasgaard & Däppen, 1992) and OPAL 2001 (Rogers et al., 1996; Rogers, 2001). OPAL comes in tabular form, but tables have also been built for the CEFF EOS (to accelerate the computation). We use an interpolation method which ensures the continuity of the first derivatives at cell boundaries in the four-dimensional space defined by the variables ρ , T , X and Z . Of course logarithmic variables are used for ρ , T , P and C_v .

Opacity:

Clés use OPAL opacities (Iglesias & Rogers, 1996, OPAL), completed by Alexander & Ferguson (1994) opacities at low temperature. Same remark as above concerning the interpolation method. The tables are four-dimensional (ρ , T , X and Z). At present time, the metal mixture is fixed within a given model. A few tables are available for different metal mixtures.

Energy generation:

The Caughlan & Fowler (1988) reaction rates have been implemented. For ${}^{14}\text{N}(p,\gamma){}^{15}\text{O}$, we use the cross-section given by Formicola et al. (2004). A version of the program uses the NACRE reaction

rates in their approximate analytical form (Angulo et al., 1999, NACRE). For the model comparison for CoRoT we used NACRE, without including the new cross-section given by Formicola for ${}^{14}\text{N}(p,\gamma){}^{15}\text{O}$.

We follow entirely the combustion of ${}^7\text{Li}$ and ${}^2\text{H}$. Only unstable species (as ${}^7\text{Be}$, ${}^{13}\text{N}$, ${}^{15}\text{O}$ and ${}^{17}\text{F}$) are supposed to be at equilibrium.

Convection:

We use the usual mixing-length theory (Böhm-Vitense, 1958), formulation by Cox & Giuli (1968). That is $\xi=1/162$, and $\Phi=9/4$. Turbulent pressure is not taken into account. There is presently some *numerical diffusion* at the boundaries of convective zones.

The implementation of convective overshoot does not use $\nabla=\nabla_{\text{ad}}$ for the temperature gradient in the overshoot layer.

Diffusion:

Diffusion has been implemented according to Thoul et al. (1994). A rather crude treatment neglecting the radiative forces is presently implemented.

Atmosphere:

The interior model is truncated at the photosphere or at an optical depth $\tau=1$, 10 or 100 according to the choice of the user and is fitted to a model atmosphere of Kurucz. A grey Eddington atmosphere (without convection) can also be fitted at the photospheric level.

1.4 FRANEC - Pisa Evolution Code [*Degl'Innocenti et al.*]

The main properties and physical assumptions of the FRANEC code are discussed in Cariulo et al. (2004) (see also Ciacio et al. 1997). For the method of integration see Chieffi & Straniero (1989).

The physical inputs are the same as the reference set for Task 1, except the adopted electronic screening which is Salpeter (1954) for weak screening, and Graboske et al. (1973) and De Witt et al. (1973) for weak-intermediate and intermediate-strong screening. The $T(\tau)$ relation is by Krishna Swamy (1966).

For the present calculations our code adopts the following reference values $L_{\odot}=3.826\times 10^{33}$ erg/s and $M_{\odot}=1.989\times 10^{33}$ g, which differ from the ones listed below.

1.5 TGEC - Toulouse-Geneva Evolution Code [*Castro*]

The details of the code are described in Charbonnel et al. (1992) and Richard et al. (1996).

The physics used in this work is the following: the EoS is from OPAL 2001 Rogers (2001), the microscopic diffusion is from Paquette et al. (1986), the opacities are OPAL 95, the nuclear energy generation is from NACRE (Angulo et al., 1999), convection is the mixing-length theory, the chemical composition is from Grevesse & Noels (1993).

The models are 1-dimensional. The star is divided in shells (the number of shells can be changed), whose thickness is variable depending on the zone: layers in transition zone between convective and radiative zones are thinner.

2 Target stars for Task 1

Seven targets have been defined. They are intended to cover a representative range in stellar masses and ages. One case has also been considered for the presence of overshoot. The reference set of physics proposed for the comparison is:

- **Equation of State** - OPAL by Rogers et al. (1996, 2001 Tables);
- **Opacities** - OPAL by Iglesias & Rogers (1996) + Alexander & Ferguson (1994);
- **Reaction rates** - NACRE by Angulo et al. (1999);
- **Convection** - MLT by Böhm-Vitense (1958), as calibrated by Henyey et al. (1965) with,

$$\alpha \equiv \frac{\ell_{\text{MLT}}}{H_p} = 1.6 ;$$

- **Overshoot** - fully mixed and $\nabla = \nabla_a$ with,

$$\alpha_{\text{ov}} \equiv \frac{\ell_{\text{ov}}}{H_p} ;$$

- **Mixture** - solar as given by Grevesse & Noels (1993);
- **Atmosphere** - grey Eddington atmosphere.

These are not necessarily the latest up-to-date specifications, but have been selected in order to form a “standard” set of physics.

The parameters for the evolution that have been specified for each case are listed in Table 1. We note that the specifications given here assume the following definitions:

- M_{HeC} is the mass of the central region of the star where the hydrogen abundance is $X \leq 0.01$.

Also indicated is the type of models that have been selected:

- **PreMS** - pre-main sequence models,
- **ZAMS** - near the beginning of the main sequence,
- **MS** - main sequence models,
- **TAMS** - near the end of the main sequence,
- **PostMS** - post-main sequence models.

In this exercise we have proposed the adoption of the following reference values:

$$M_{\odot} = 1.98919 \times 10^{33} \text{ g and } (GM)_{\odot} = 1.32712438 \times 10^{26} \text{ cm}^{-3} \text{ s}^{-2},$$

$$R_{\odot} = 6.9599 \times 10^{10} \text{ cm},$$

$$L_{\odot} = 3.846 \times 10^{33} \text{ erg s}^{-1}.$$

3 Comparison: global parameters

The global parameters for the models calculated by the different codes, following the specifications listed in Table 1, are given in Table 2 for models in the main sequence (Cases 1.1, 1.2, 1.6 and 1.7) and in Table 3 for models off the main sequence (Cases 1.3, 1.4 and 1.5). The largest difference in the parameters (Δ_{max}) is also given in the tables in order to illustrate the magnitude of the discrepancy in each parameter.

The reference set of physics has not been fully implemented in all codes. Consequently part of the differences found in both Tables (2 and 3) are consequence of the differences in the physics used for the calculations.

4 Comparison: internal structure

With a preliminary comparison of two functions of the internal structure we aim at providing an indication on where potential difficulties may be. As two representative functions we have selected the sound speed (shown in Figs 1 and 2) and the abundance of hydrogen (shown in Figs 3 and 4).

In this exercise we have already iterated in order to reduce the relative differences. But in some cases further work will need to be done, and in particular the models will have to be calculated following the specifications as some of the differences are yet due to the use of a different set of physics.

5 Discussion

It is shown here that the models calculated by five different codes are - to first order - consistent, as one would expect. The relative differences in the global parameters, listed in Tables 2 and 3, are small. The specifications for the targets have not been precisely followed and the reference set of physics defined for this exercise is also not fully implemented in some of the codes. Those are the two major reasons why there is a difference in the values of the global parameters (R, L, T_{eff}) found here. This will be addressed in the improvement of these preliminary results we are reporting here.

The differences of the internal structure, as seen in the squared sound speed and the abundance of hydrogen, have also been shown for those models. Given the differences of the global parameters describing the solutions being compared, the differences in the internal structure reported here can be considered as “expectable”. However we have found that for some cases clear differences, in particular complex regions of the star, can be seen between different codes. Such problematic regions are a clear illustration of where the implementation of the physics must still be carefully analysed. An effort on clarifying how some of these aspects can be represented in the calculations will be pursued as a next step to the preliminary analysis shown here.

References

- Alexander, D. R. & Ferguson, J. W., 1994, ApJ, **437**, 879
- Angulo, C., Arnould, M. & the NACRE collaboration, 1999, Nuclear Physics A, **656**, 3
- Bahcall, J. N. & Pinsonneault, M. H., 1995, Rev. Mod. Phys., **67**, 781
- Böhm-Vitense, E., 1958, *Z. Astrophys.*, **46**, 108
- Cariulo, P., Degl'Innocenti, S., Castellani, V., 2004, A&A, **421**, 1121
- Caughlan, G. R., Fowler, W. A., 1988, Atomic data and nuclear tables, **40**, 283
- Charbonnel, C., Vauclair, S. & Zahn, J.-P., 1992, A&A, **255**, 191
- Chieffi & Straniero, 1989, ApJS, **71**, 47
- Christensen-Dalsgaard, J., 1978, *Solar oscillations, PhD Dissertation*, University of Cambridge
- Christensen-Dalsgaard, J., 1982, MNRAS **199**, 735
- Ciacio, F., degl'Innocenti, S. & Ricci, B., 1997, A&AS, **123**, 449
- Cox, J. P. & Giuli, R. T., 1968, *Principles of Stellar Structure, Vol II: Application to Stars*, Gordon and Breach
- Christensen-Dalsgaard, J., W. Däppen, 1992, A&A, **4**, 267
- De Witt, Graboske & Cooper, 1973, ApJ, **181**, 439
- Formicola et al., 2004
- Graboske et al., 1973, ApJ, **181**, 457
- Grevesse, N. & Noels, A., 1993, in *La Formation des Éléments Chimiques*, R. D. Harck & S. Paltani (eds)
- Heney, L. G., Vardya, M. S. & Bodenheimer, P., 1965, ApJ, **142**, 841
- Iglesias, C. A. & Rogers, F. J., 1996, ApJ, **464**, 943
- Krishna Swamy, K. S., 1966, ApJ, **145**, 174
- Kurucz Tables at <http://kurucz.harvard.edu/>
- Morel P., 1997, A&A, **124**, 597
- NACRE Project, at <http://pntpm.ulb.ac.be/Nacre/nacre.htm>
- OPAL Project, at <http://www-phys.llnl.gov/Research/OPAL/index.html>
- Paquette, C., Pelletier, C., Fontaine, G. & Michaud, G., 1986, ApJS, **61**, 177
- Richard, O., Vauclair, S., Charbonnel, C. & Dziembowski, W. A., 1996, A&A, **312**, 1000
- Rogers, F. J., 2001, Contributions to plasma physics, **41**, 179
- Rogers, F. J., Swenson, F. J. & Iglesias, C. A., 1996, ApJ, **456**, 902
- Thoul A., Bahcall, J. N. & Loeb, A., 1994, ApJ, **421**, 828
- Salpeter, 1954 Australian J. Phys., **7**, 373

Table 1: Description of the target models proposed under Task 1 of the ESTA/CoRoT Model Comparison project. The standard symbols are used. The mass (M), radius (R), luminosity (L) and the He core mass (M_{HeC}) are in solar units ($M_{\odot}, R_{\odot}, L_{\odot}$), while the mixing length (ℓ_{MLT}) and the overshoot factor (ℓ_{ov}) are in pressure scale heights (H_p).

Cases:	1.1	1.2	1.3	1.4	1.5	1.6	1.7
Parameters:							
M/M_{\odot}	0.9	1.2	1.2	2.0	2.0	3.0	5.0
X_0	0.70	0.70	0.73	0.70	0.72	0.71	0.70
Y_0	0.28	0.28	0.26	0.28	0.26	0.28	0.28
Z_0	0.02	0.02	0.01	0.02	0.02	0.01	0.02
ℓ_{MLT}/H_p	1.6	1.6	1.6	1.6	1.6	1.6	1.6
ℓ_{ov}/H_p	0.0	0.0	0.0	0.0	0.15	0.0	0.0
Target models:							
X_c	0.35	0.69	-	-	0.01	0.69	0.35
T_c	-	-	-	1.9×10^7	-	-	-
M_{HeC}/M_{\odot}	-	-	0.1	-	-	-	-
Type:	MS	ZAMS	PostMS	PreMS	TAMS	ZAMS	MS

Table 2: Global parameters for the models in the main sequence calculated using different stellar evolutionary codes. The standard symbols are used. Age is in Myrs, while mass (M), radius (R) and luminosity (L) are in solar units ($M_{\odot}, R_{\odot}, L_{\odot}$). The temperatures and density are in CGS. The mass of convective cores (M_{cor}) and the radii of external convective zones (R_{env}) are in stellar units. The value of X_c is the parameter used to specify the target model.

	Age	$\frac{R}{R_{\odot}}$	$\frac{L}{L_{\odot}}$	T_{eff}	$\frac{T_c}{10^7}$	ρ_c	X_c	$\frac{M_{\text{cor}}}{M}$	$\frac{R_{\text{env}}}{R}$
Case 1.1:									
ASTEC	6745	0.8927	0.6237	5434	1.443	150.5	0.3500	-	0.6954
CESAM ₀	6782	0.8916	0.6262	5443	1.448	150.9	0.3501	-	0.6958
CESAM ₁	6886	0.8933	0.6237	5432	1.444	150.0	0.3500	-	0.6957
CLES	6816	0.8954	0.6245	5428	1.447	151.2	0.3496	-	0.6972
FRANEC	6592	0.9114	0.6522	5431	1.461	153.4	0.3500	-	0.7027
TGEC	6554	0.8945	0.6510	5490	1.458	154.2	0.3491	-	0.7013
Δ_{max}	0332	0.0198	0.0285	0062	0.018	004.2	0.0010	-	0.0073
Case 1.2:									
ASTEC	074.4	1.151	1.789	6227	1.578	86.69	0.6900	0.0106	0.8288
CESAM ₀	096.7	1.146	1.776	6231	1.577	86.65	0.6900	0.0087	0.8265
CESAM ₁	080.8	1.147	1.775	6226	1.575	86.46	0.6900	0.0087	0.8282
CLES	098.5	1.146	1.778	6232	1.577	86.68	0.6900	0.0094	0.8292
FRANEC	097.2	1.183	1.859	6194	1.590	87.35	0.6900	0.0101	0.8497
TGEC	105.9	1.148	1.849	6290	1.589	88.31	0.6900	0.0095	0.8422
Δ_{max}	031.5	0.037	0.084	0096	0.015	01.85	0.0000	0.0019	0.0232
Case 1.6:									
ASTEC	13.71	1.864	101.5	13432	2.479	42.68	0.6900	0.2129	0.9990
CESAM ₀	14.47	1.854	101.4	13466	2.486	43.04	0.6901	0.2114	0.9945
CESAM ₁	14.04	1.854	101.4	13470	2.486	43.05	0.6900	0.2114	0.9945
CLES	14.76	1.852	101.6	13479	2.487	43.08	0.6900	0.2104	0.9938
FRANEC	14.86	1.863	104.5	13517	2.488	42.48	0.6894	0.2106	0.9940
Δ_{max}	01.15	0.012	003.1	00085	0.009	00.60	0.0007	0.0025	0.0052
Case 1.7:									
ASTEC	56.88	3.905	748.2	15291	2.829	19.49	0.3500	0.1600	0.9996
CESAM ₀	55.94	3.854	739.6	15348	2.836	19.76	0.3498	0.1567	0.9943
CESAM ₁	55.58	3.852	739.4	15350	2.836	19.77	0.3500	0.1568	0.9943
CLES	56.39	3.865	741.8	15337	2.837	19.77	0.3500	0.1564	0.9932
FRANEC	54.73	3.904	772.3	15395	2.844	19.54	0.3496	0.1638	0.9928
Δ_{max}	02.15	0.053	032.9	00104	0.015	00.27	0.0004	0.0074	0.0068

Table 3: Global parameters for the models off the main sequence calculated using different stellar evolutionary codes. The standard symbols are used. Age is in Myrs, while mass (M), mass of the helium core (M_{HeC}), radius (R) and luminosity (L) are in solar units ($M_{\odot}, R_{\odot}, L_{\odot}$). The temperatures and density are in CGS. The mass of convective cores (M_{cor}) and the radii of external convective zones (R_{env}) are in stellar units. The value with the box indicates the parameter that has been used to specify the target model.

	Age	$\frac{R}{R_{\odot}}$	$\frac{L}{L_{\odot}}$	T_{eff}	$\frac{T_c}{10^7}$	ρ_c	X_c	$\frac{M_{\text{HeC}}}{M_{\odot}}$	$\frac{M_{\text{cor}}}{M}$	$\frac{R_{\text{env}}}{R}$
Case 1.3:										
ASTEC	4314	2.164	5.513	6019	2.183	3276	-	0.1000	-	0.7794
CESAM ₁	4552	2.164	5.582	6037	2.187	3206	-	0.1000	-	0.7824
CLES	4401	2.170	5.617	6038	2.205	3210	-	0.1000	-	0.7843
FRANEC	4207	2.275	5.808	5939	2.203	3205	-	0.1014	-	-
Δ_{max}	0345	0.111	0.295	0099	0.022	0071	-	0.0014	-	0.0030
Case 1.4:										
CESAM ₀	7.043	1.866	15.80	8431	1.900	49.22	0.6994	-	0.1075	0.9988
CESAM ₁	6.643	1.871	15.97	8444	1.900	49.01	0.6994	-	0.1148	0.9918
CLES	7.716	1.875	16.23	8469	1.900	50.17	0.6993	-	0.0927	0.9915
FRANEC	7.798	1.879	16.50	8484	1.900	49.11	0.6994	-	0.0957	0.9986
Δ_{max}	1.155	0.013	01.50	0053	0.000	01.16	0.0001	-	0.0221	0.0007
Case 1.5:										
ASTEC	1174	3.542	22.62	6695	2.784	130.5	0.0100	-	0.0778	0.9872
CESAM ₀	1185	3.543	22.91	6715	2.794	131.8	0.0100	-	0.0770	0.9870
CESAM ₁	1173	3.537	22.87	6718	2.795	131.8	0.0100	-	0.0770	0.9871
CLES	1209	3.634	23.38	6665	2.800	131.7	0.0100	-	0.0770	0.9862
Δ_{max}	0036	0.097	00.76	0053	0.016	001.3	0.0000	-	0.0008	0.0010

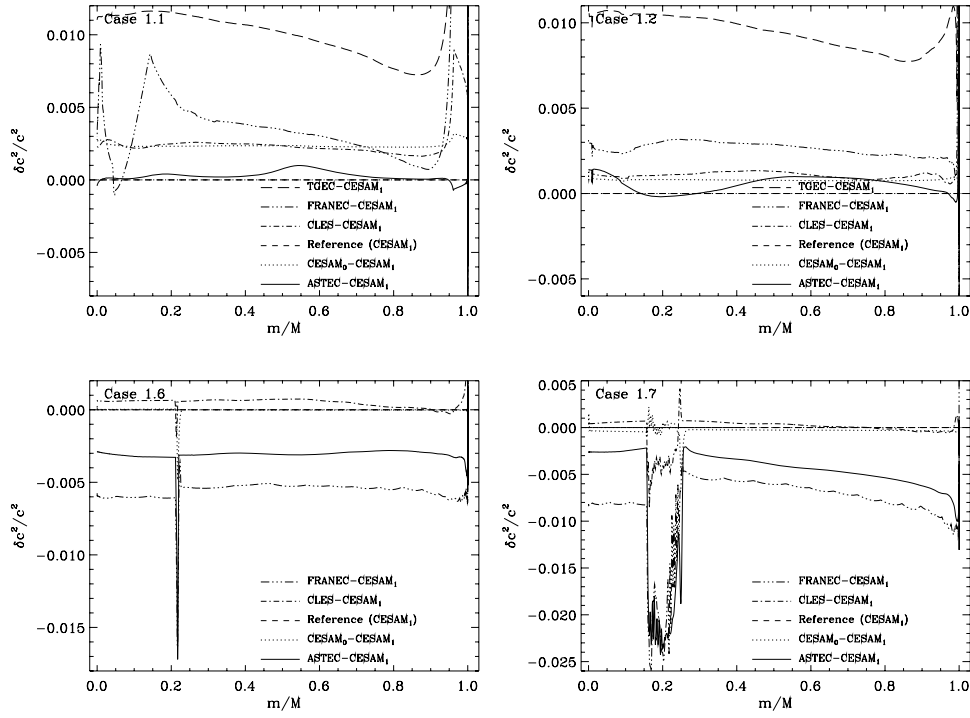


Figure 1: Plot of the sound speed differences (at fixed relative mass) between pairs of models in the main sequence (see Table 2). The panels are for Cases 1.1, 1.2, 1.6 and 1.7, as indicated.

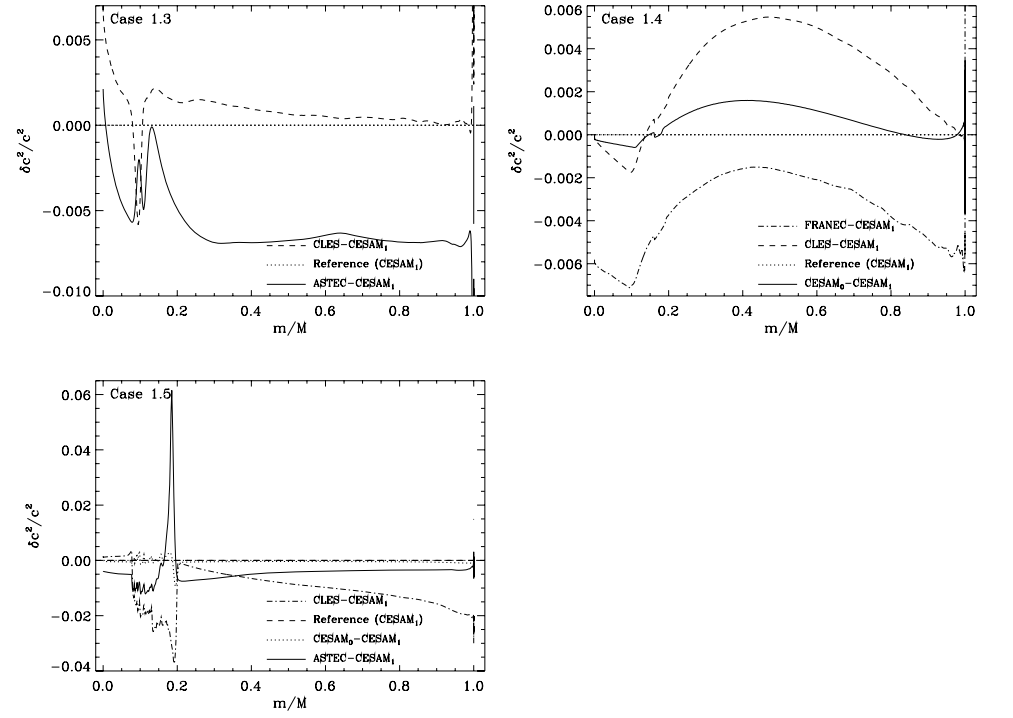


Figure 2: Plot of the sound speed differences (at fixed relative mass) between pairs of models off the main sequence (see Table 3). The panels are for Cases 1.3, 1.4 and 1.5 as indicated.

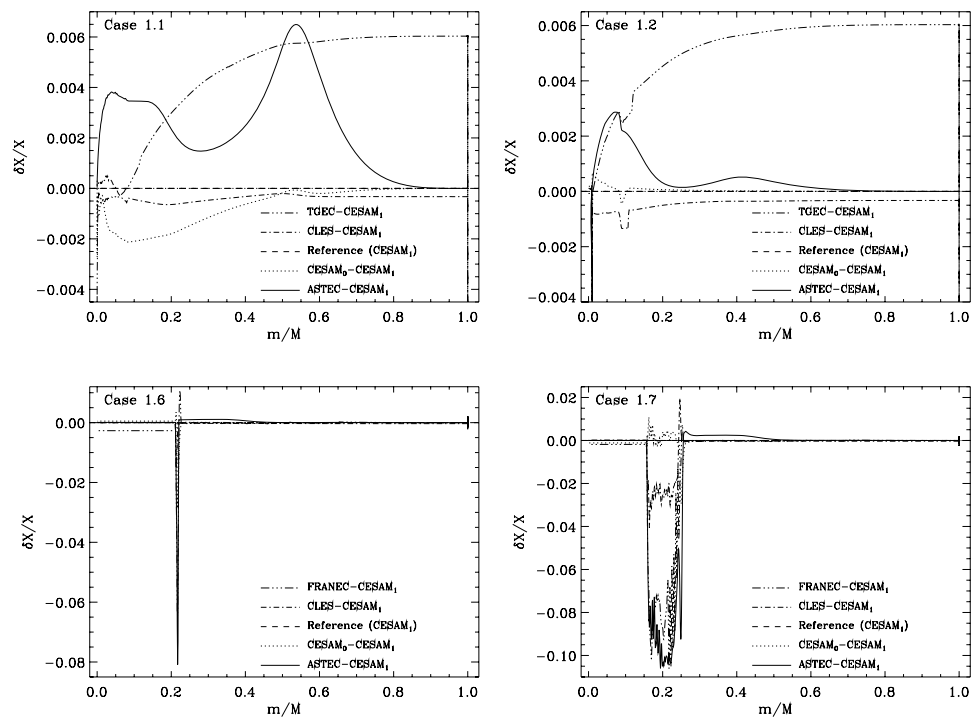


Figure 3: Plot of the hydrogen abundance differences (at fixed relative mass) between pairs of models in the main sequence (see Table 2). The panels are for Cases 1.1, 1.2, 1.6 and 1.7, as indicated.

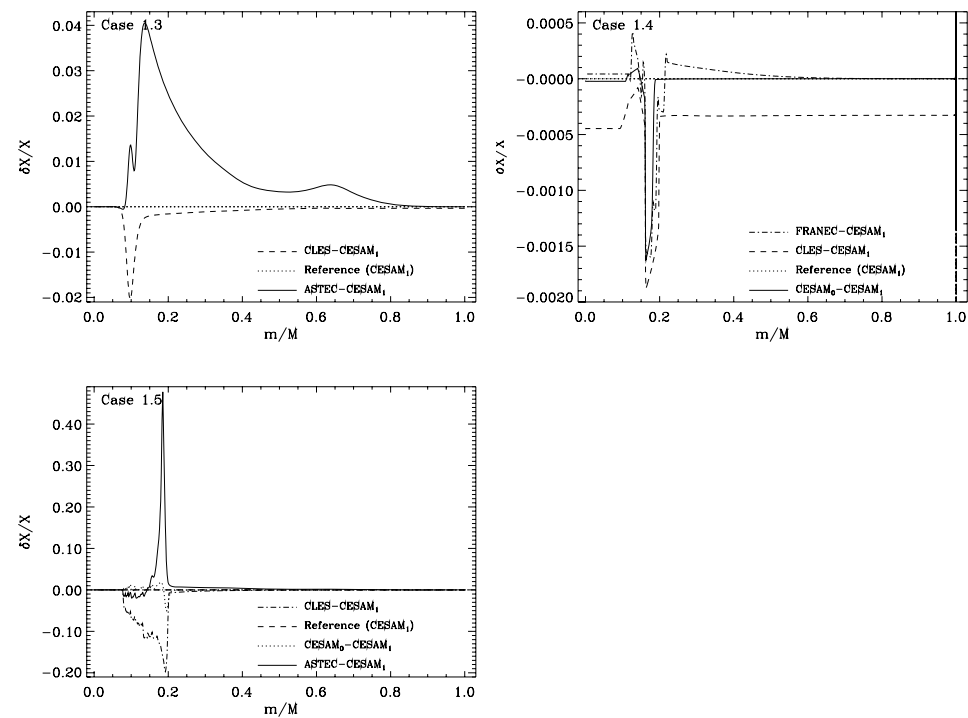


Figure 4: Plot of the hydrogen abundance differences (at fixed relative mass) between pairs of models off the main sequence (see Table 3). The panels are for Cases 1.3, 1.4 and 1.5 as indicated.